*Pol. J. Environ. Stud. Vol. 31, No. 5 (2022), 4975-4983*
DOI: *10.15244/pjoes/150082* ONLINE PUBLICATION DATE: 2022-08-08

*Original Research*

# Effect of Incorporation of Pectin on the Adsorption of Phosphate by Al (oxy)hydroxides

**Xiaofang Zhu[1, 3], Ping Wang[1]*, Jun Jiang[2], Ruhai Wang[2]**, Renkou Xu[2], Yuanchun Yu[1]**

[1]College of Biology and the Environment, Nanjing Forestry University, Nanjing 210037, People's Republic of China
[2]State Key Laboratory of Soil and Sustainable Agriculture, Institute of Soil Science, Chinese Academy of Sciences, Nanjing 210008, People's Republic of China
[3]Nanjing Institute of Product Quality Inspection, Nanjing 210028, People's Republic of China

*Received: 4 April 2022*
*Accepted: 16 May 2022*

## Abstract

The structural and surface charge properties of Al (oxy)hydroxides formed in the presence of pectin, as well as the effect of incorporating pectin on phosphate adsorption by Al (oxy)hydroxides, are examined in this study. Results indicate that pectin entered the structure of the Al (oxy)hydroxides during their formation, which inhibited crystallization of Al hydrolysis products. The incorporation of pectin decreased the surface positive charge on the Al (oxy)hydroxides and the point of zero charge of hydroxides. The amount of phosphate adsorbed by Al hydrolysis products incorporating pectin was considerably higher than that adsorbed on products without pectin at the same pH within the range 4.5-6.0. The maximum adsorption capacity of phosphate on Al (oxy)hydroxides increased from 134.7 mmol $kg^{-1}$ for that formed without pectin to 248.2 mmol $kg^{-1}$ for that formed by incorporation of pectin at an initial pectin/Al loading ratio of 20 mg $mmol^{-1}$. Adsorption kinetics indicated that the incorporation of pectin decreased the rate constant and increased the maximum adsorption capacity of phosphate on the surface of Al (oxy)hydroxides. In conclusion, incorporation of pectin affects the surface properties of Al (oxy)hydroxides and leads to an increase in adsorption of phosphate.

**Keywords**: Al (oxy)hydroxides, incorporation of pectin, phosphate adsorption, short-range order, surface properties

## Introduction

Large amounts of phosphate-containing fertilizer are widely applied to support intensive agricultural production [1, 2]. It is estimated that globally about $3\times10^6$–$4\times10^6$ tons of $P_2O_5$ migrates from soil to water annually, including about 19.5 kg $ha^{-1}$ from farmland in China [3]. Therefore, management and control of phosphate in agricultural activities is essential for overall ecosystem health [4, 5].

Typically, phosphate can be readily adsorbed and immobilized by soil minerals such as iron and aluminum compounds [6]. On the other hand, anion and organic materials adsorbed on the surface of Al hydrolysis products can dissipate the positive charge at

*e-mail: hgwp@njfu.edu.cn
**e-mail: rhwang@issas.ac.cn

the metal center, thereby reducing anionic adsorption [7]. Xu et al. showed that arsenate reduced phosphate uptake by aluminum hydroxides through competition with anions for adsorption sites [8].

However, in contrast to organic matter adsorbed on the surface, the incorporation of organic material into Al hydrolysis products enhances anion adsorption thereon [9]. Kwong and Huang found that the incorporation of citric acid into Al hydrolysis products increased phosphate adsorption [10]. Many soil/sediment-forming factors, such as the organic materials humic acid [11] and tannic acid [12], and low molecular weight organic compounds [13], can perturb the formation of Al (oxy) hydroxides, resulting in the formation and stabilization of short-range order Al (oxy)hydroxides [14]. Due to structural defects, high specific surface area and charge density, and resultant high surface reactivity, short-range order Al (oxy)hydroxides formed under the influence of organic ligands are much more reactive in comparison to their crystalline counterparts [10, 15, 16]. This reactive nature is attributed to increased removal of surface-bound $H_2O$ by organic ligands, and/or adsorption of organic ligands on the Al (oxy)hydroxides, resulting in increased development of negative charge on their surfaces [9].

Variable-charge soils are acidic, with soluble Al and exchangeable Al being the most active components of Al pools therein [17]. Hydrolysis of active Al in soil occurs when acidic soils are ameliorated with alkaline materials; pure Al hydrolysis products rarely exist in natural environments [18]. Pectin is present in most primary cell walls of plant roots, particularly in root tips [19], and it can be extracted from suitable agricultural by-products, such as citrus peel [20]. It has a high cation-exchange capacity due to the presence of carboxyl, aldehyde, and hydroxyl functional groups [21]. Pectin secreted from plant roots affects the chemical properties of soil and minerals [22, 23]. It is assumed that pectin may take part in Al hydrolysis reactions, similar to other organic materials, and thus affect the structural and surface properties of Al hydrolytic products.

To the best of our knowledge, there have not hitherto been any reports on the incorporation of pectin into Al hydrolysis products and its effect on phosphate adsorption. The main objectives of this study, therefore, are: (1) to examine the structural and surface charge properties of Al (oxy)hydroxides formed by incorporating pectin, and (2) to evaluate the effect of incorporated pectin on the adsorption of phosphate by Al (oxy)hydroxides.

## Material and Methods

### Chemicals

Citrus pectin powder, partially consisting of methoxylated polygalactouronic acid, was provided by Sigma Chemical Co. The galactouronic acid content was about 740 g $kg^{-1}$ and the carbon content of the pectin was 365 g $kg^{-1}$. $NaH_2PO_4$ and $NaNO_3$ (both analytical grade) and deionized water were used for all experiments. An Na-pectin stock solution (pectin 420 mg $L^{-1}$) was prepared by first dissolving pectin (2.100 g) in deionized water (5.0 L) with the aid of magnetic stirring for 6 h. This pectin solution w as then titrated to pH 6.0 with 0.1 mol $L^{-1}$ NaOH solution.

### Synthesis of Al (oxy)hydroxides

Al (oxy)hydroxides were synthesized using the method reported by Yu et al. [14], whereby $AlCl_3$ solution with or without pectin was slowly titrated with 0.1 mol $L^{-1}$ NaOH solution under vigorous stirring. In summary, a 3.0 L aliquot of 7.0 mmol $L^{-1}$ $AlCl_3$ solution was titrated with a 0.1 mol $L^{-1}$ NaOH solution in a 5.0 L beaker until pH 4.8 was reached. With or without the addition of 1.0 L of 420 mg $L^{-1}$ Na-pectin solution, the $AlCl_3$ solution was then further titrated with 0.1 mol $L^{-1}$ NaOH at a rate of 2.5 mL $min^{-1}$ until an OH/Al molar ratio of 3.0 was achieved (initial loading ratio of pectin/Al of 20 mg $mmol^{-1}$). The suspensions of all reaction systems were aged for 45 days at room temperature. After aging, the suspensions were centrifuged, the supernatants were removed, and the Al (oxy)hydroxides were washed with deionized water until the electrical conductivity of the filtrate was lower than 5 μS/cm. The Al (oxy)hydroxides were finally freeze-dried before analysis.

### Characterization of Al (oxy)hydroxides

Al (oxy)hydroxides (30 mg) were digested in 6 mol $L^{-1}$ hydrochloric acid (10.0 mL), and then solutions were diluted to a constant volume of 100 mL. The concentration of Al was measured by inductively coupled plasma-optical emission spectrometry (ICP-OES; Optima 8000, Perkin-Elmer, Waltham, MA, USA). Carbon contents were determined using an elemental analyzer (Vario Max CN, Elementar, Germany). The mineralogical components of the formed Al (oxy)hydroxides were identified by X-ray diffraction (XRD) analysis (Ultima IV, Rigaku Industrial Corporation, Japan), employing Cu-$K_\alpha$ radiation filtered by a graphite monochromator and operating at 40 kV and 40 mA. XRD patterns were recorded from 4° to 60° at a scanning rate of 2° $min^{-1}$ in continuous mode. A surface morphological study of the samples was undertaken using an environmental scanning electron microscope (SEM; Quanta 200, FEI, Netherlands). Fourier-transform infrared (FTIR) spectra of the formed Al (oxy)hydroxides were recorded on a Nicolet is10 spectrophotometer (Thermo Fisher Scientific, USA), scanning from 400 to 4000 $cm^{-1}$ at a resolution of 4 $cm^{-1}$.

### Surface Charge Measurement

The surface charge of Al (oxy)hydroxides was determined by titration experiment [24]. Briefly, an aliquot of 50 mL of 1.0 mmol $L^{-1}$ or 100 mmol $L^{-1}$ $NaNO_3$ solution was placed in a 100 mL polyethylene bottle containing 0.200 g of Al (oxy)hydroxides. The suspension was then titrated to pH 4.5 using 0.1 M $HNO_3$. After equilibration for 30 min, the suspension was titrated to pH 11 using 0.1 M NaOH solution at 25ºC with an automatic potentiometric titrator (Metrohm 862, Switzerland). In order to ensure that atmospheric $CO_2$ did not enter the system, all titration experiments were conducted under $N_2$. $OH^-$ uptake recorded for blank samples was subtracted from the results for the suspensions to remove potential contamination errors. The points of zero salt effect (PZSE) of Al (oxy) hydroxides were obtained from the intersections of the two titration curves in 1.0 and 100 mmol $L^{-1}$ $NaNO_3$ solutions. The net surface charge was calculated from the amount of $OH^-$ adsorbed relative to the PZSE.

### Phosphate Adsorption Batch Experiments

Al (oxy)hydroxides formed with and without the incorporation of pectin were selected for batch adsorption experiments. Al (oxy)hydroxides (0.200 g each) were placed in 80 mL polyethylene bottles. Aliquots of 2.5 mmol $L^{-1}$ $NaNO_3$ solution (10 mL) and $NaH_2PO_4$ solutions (15 mL) of various concentrations were then added to each bottle. In order to study the effect of pH, the initial concentration of phosphate was 3.0 mmol $L^{-1}$. Phosphate adsorption isotherms were studied with initial phosphate concentrations of 0.5, 1.0, 1.5, 2.0, 2.5, 3.0, and 4.0 mmol $L^{-1}$ at pH 5.5. The polyethylene bottles were then shaken for 6 h in a constant-temperature water bath set at 25±1ºC. During this period, the pH of the suspension was checked at least twice, and adjusted if necessary, to meet the target pH value. The suspensions were then left to stand overnight before being centrifuged at 13583 *g* for 5 min. The samples were then filtered through a 0.45 μm membrane filter. The concentration of phosphorus in the solutions was determined by ICP-OES. The amount of phosphate adsorbed by the Al (oxy) hydroxides was calculated from the difference between the total amount added and the amount remaining in solution.

### Kinetic Experiments on Phosphate Adsorption

The kinetics of phosphate adsorption by Al (oxy) hydroxides formed with and without incorporation of pectin was studied by the conventional method. Al (oxy)hydroxides (2.0 g) was placed in a 500 mL glass beaker. An aliquot (250 mL) of a solution containing 3.0 mM $NaH_2PO_4$ and 1.0 mM $NaNO_3$ was then added and the mixture was magnetically stirred at 450 rpm. At various intervals, a 2 mL aliquot of the suspension was withdrawn and filtered through a 0.45 μm membrane filter within 15 s using an injector. The phosphate concentration and pH of the filtrate were measured by using ICP-OES and a pH meter, respectively. The amount of phosphate adsorbed was determined based on the difference between the initial concentration and the fraction remaining in solution. The amount of phosphate adsorbed at time $t$, $q_t$ (mmol $kg^{-1}$), was calculated according to Eq. (1):

$$q_t = (C_0 - C_t) \times V/m \quad (1)$$

where $C_0$ and $C_t$ are the liquid-phase concentrations (mmol $L^{-1}$) initially and at time $t$, respectively, $V$ is the volume (mL) used for the kinetic experiments, and $m$ (g) is the mass of Al (oxy)hydroxides added.

## Results and Discussion

### Characterization of Al (oxy)hydroxides

The incorporation of pectin resulted in a decrease in the total Al content of the Al (oxy)hydroxides from 331 to 252 g $kg^{-1}$. The organic carbon content in the Al (oxy) hydroxides with pectin incorporation was 67.3 g $kg^{-1}$.

XRD patterns of Al (oxy)hydroxides with and without the incorporation of pectin are presented in Fig. 1. The results indicated that Al (oxy)hydroxides formed in the absence of pectin was dominated by crystalline gibbsite and bayerite. When Al (oxy) hydroxides were formed in the presence of pectin, the gibbsite peaks were no longer seen, and those of bayerite were greatly diminished compared to those for the sample without pectin. The decrease in peak intensity indicated that the bayerite was less crystalline, smaller in size, and/or present at a lower level. This result indicated that pectin interfered with the formation of crystalline Al (oxy)hydroxides, a finding in accordance with those of Xu et al. [13] and Hu et al. [12], who observed perturbation of the crystallization of Al (oxy)hydroxides with varying concentrations of low molecular weight organic acids/humic acid and tannic acid, respectively.

Images acquired by SEM provided insight into Al hydrolysis products formed under conditions with and without pectin (Fig. 2). SEM analysis has previously been used to characterize crystalline or non-crystalline Al hydrolysis products [11]. In terms of size, Al (oxy)hydroxides formed in the absence of pectin had a smaller diameter and were crystalline; Al hydrolysis products incorporating pectin were larger and only contained a small amount of crystals on their surfaces. These results are consistent with those obtained by XRD.

FTIR spectra of pectin and of Al (oxy)hydroxides formed with or without pectin (Fig. 3) feature a band at 1745 $cm^{-1}$ attributable to the C=O stretching

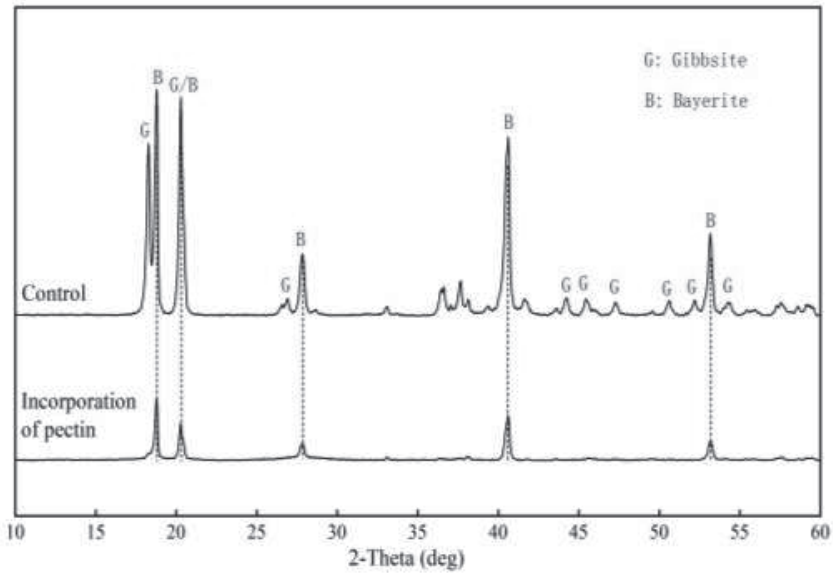


Fig. 1. X-ray diffraction patterns of Al (oxy)hydroxides formed without (control) and with incorporation of pectin.

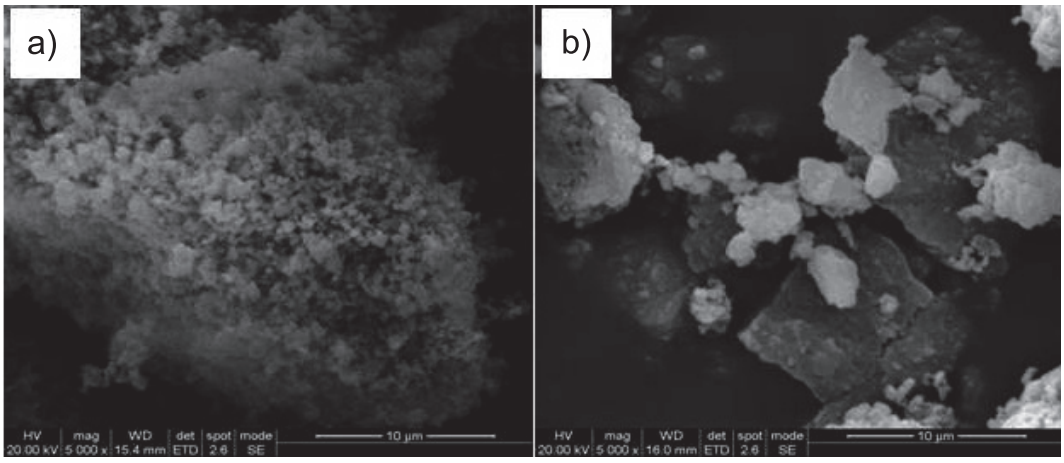


Fig. 2. Scanning electron micrographs of Al (oxy)hydroxides formed without a) and with b) incorporation of pectin.

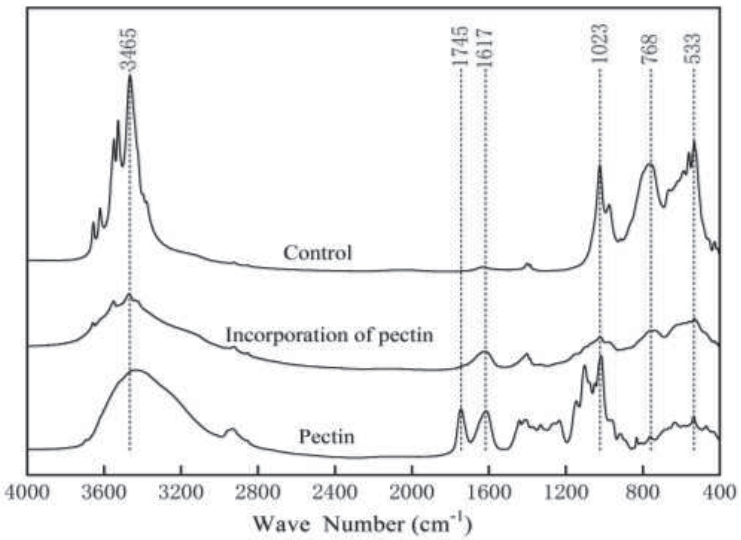


Fig. 3. FTIR spectra of pectin and Al (oxy)hydroxides formed without (control) and with incorporation of pectin.

vibration of the carbomethoxy group, and a band at 1617 $cm^{-1}$ attributable to the asymmetric stretching vibration of carboxylate [25]. The fingerprint region of pectin features characteristic bands at 1235, 1102, and 1017 $cm^{-1}$ [26]. In the spectrum of the Al (oxy) hydroxides product obtained without pectin, the band at 3465 $cm^{-1}$ can be assigned to hydroxyl stretching, and the fingerprint region comprises bands at 1023, 768, and 533 $cm^{-1}$ [14]. The spectra of samples incorporating pectin showed a broad peak at 3465 $cm^{-1}$, attributable to the formation of noncrystalline Al (oxy)hydroxides [27]. The peak at 1617 $cm^{-1}$ in the spectrum of pectin-incorporating Al (oxy)hydroxides can be assigned to the asymmetric stretching vibration of carboxylate in pectin, verifying the envisaged incorporation [28]. No shift was observed in the position of this peak at 1617 $cm^{-1}$, possibly indicating the presence of some free pectin in the Al (oxy)hydroxides.

## Surface Charge of Al hydroxides

The changes in surface charge of the Al hydrolysis products with and without incorporation of pectin are presented in Fig. 4. With an increase of pH, the surface positive charge of the Al hydrolysis product decreased. The incorporation of pectin also led to a decrease in the surface positive charge on the Al (oxy)hydroxides (Fig. 4). For example, at pH 5.0, the positive surface charge on Al (oxy)hydroxides was decreased from 516 mmol $kg^{-1}$ for the control to 185 mmol $kg^{-1}$ for the pectin-incorporating sample. The PZSE values of Al (oxy)hydroxides with and without pectin were obtained from the intersection of two curves of their surface charge with changing pH in 1.0 and 100 mmol $L^{-1}$ $NaNO_3$ solutions. The incorporation of pectin decreased the PZSE of Al hydrolysis products from 10.5 to 9.3 (Fig. 4). A similar effect of tannate on the PZSE of Al (oxy)hydroxides was reported by Yu et al [14]. They found that the PZSE of Al (oxy)hydroxides formed under the influence of tannate substantially decreased with an increase in the initial tannate/Al molar ratio. This change was attributed to increased removal of surface-bound $H_2O$ from the Al (oxy)hydroxides by organic materials through co-precipitation and/or adsorption, resulting in more exposure of the $COO^-$ groups of organic materials, and increased development of negative charge on the surfaces of the materials.

## Effect of pH on Phosphate Adsorption

The adsorption of phosphate on Al (oxy)hydroxides formed with or without pectin was seen to decrease with increasing pH (Fig. 5). This change can be mainly attributed to increasing negative charge on the surfaces of the Al hydrolysis products (Fig. 4). For example, when the pH was increased from 5.25 to 7.05, the amount of phosphate adsorbed by Al (oxy) hydroxides incorporating pectin decreased from 234.2 to 148.5 mmol $kg^{-1}$. Our results also indicated that the amount of phosphate adsorbed by Al hydrolysis products incorporating pectin was much greater than that adsorbed by Al hydrolysis products without pectin at the same pH within the range 4.5-7.0 (Fig. 5). At pH 6.0, the amount of phosphate adsorbed by Al hydrolysis product incorporating pectin was 187.0 mmol $kg^{-1}$, as compared with only 102.5 mmol $kg^{-1}$ for the Al hydrolysis product formed without pectin, an increase of 82.4%.

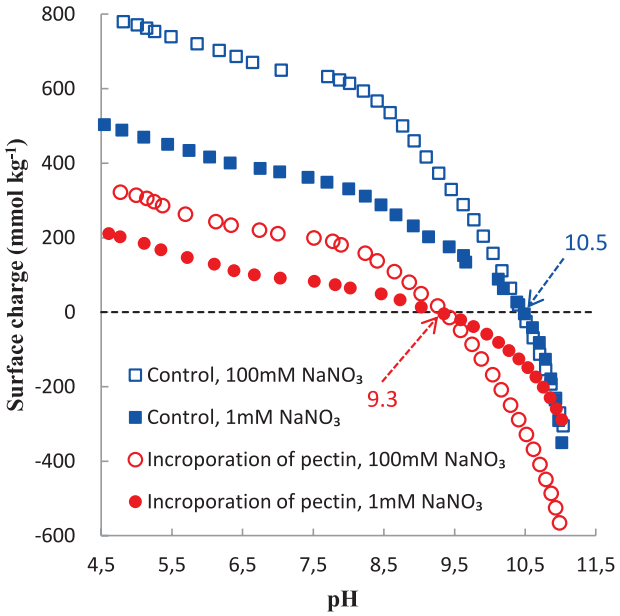


Fig. 4. Surface charges of Al (oxy)hydroxides formed without (control) and with incorporation of pectin in 1 mmol $L^{-1}$ (solid points) and 100 mmol $L^{-1}$ $NaNO_3$ (hollow points) solutions at different pH levels, as determined using an acid–base titration method.

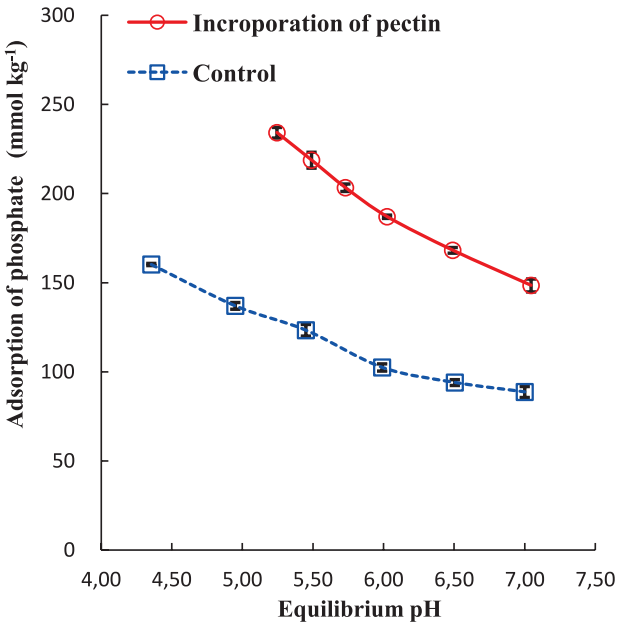


Fig. 5. Phosphate adsorption by Al (oxy)hydroxides formed without (control) and with incorporation of pectin at different pH levels (initial concentration of phosphate 3.0 mmol $L^{-1}$).

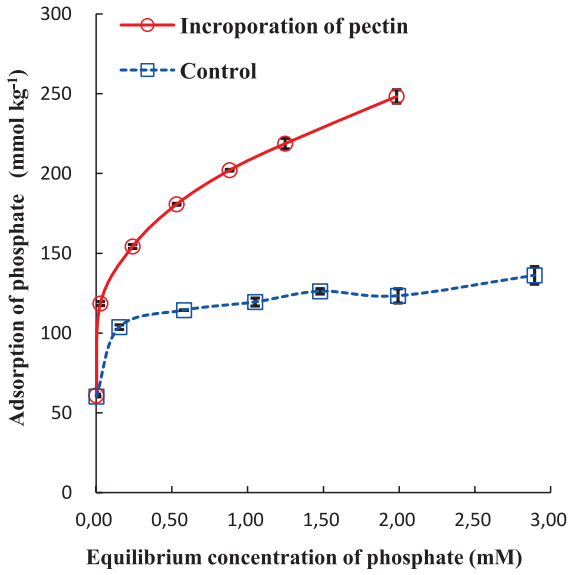


Fig. 6. Adsorption isotherms of phosphate on Al (oxy)hydroxides formed without (control) and with incorporation of pectin at pH 5.5 (initial concentrations of phosphate 0.5, 1.0, 1.5, 2.0, 2.5, 3.0, and 4.0 mmol $L^{-1}$, respectively).

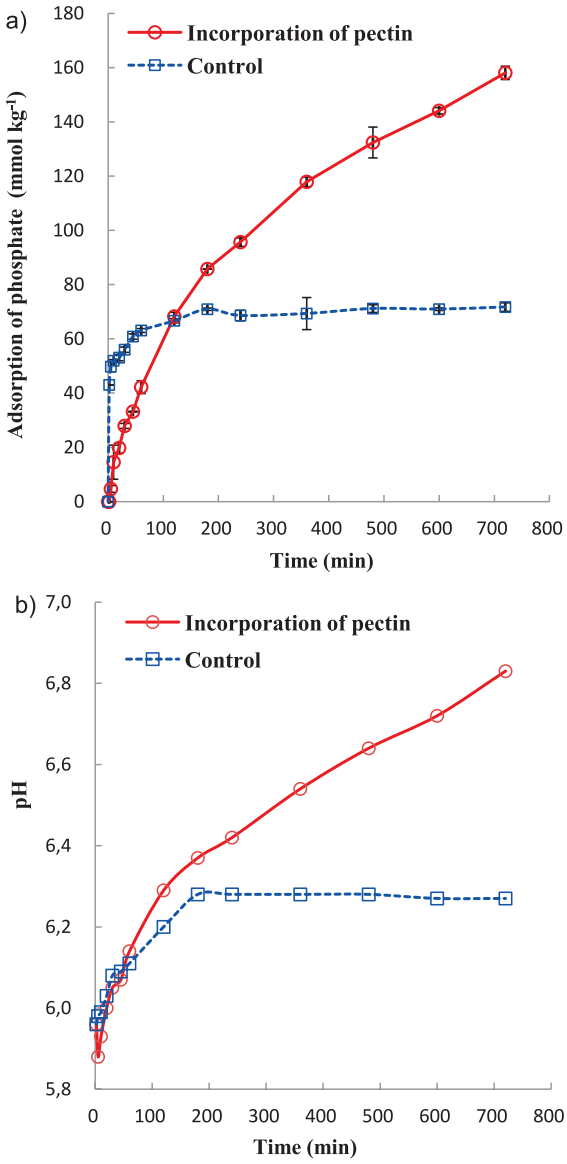


Fig. 7. Adsorption kinetics of phosphate on Al (oxy)hydroxides formed without (control) and with incorporation of pectin a) by the conventional method and pH of solution during this process b) (initial concentration of phosphate 3.0 mmol $L^{-1}$).

## Phosphate Adsorption Isotherms

Adsorption isotherms of phosphate on Al (oxy) hydroxides formed with and without pectin indicated that phosphate adsorption increased with an increase in equilibrium concentration (Fig. 6). Pectin incorporation increased the amount of phosphate adsorbed on Al (oxy) hydroxides at various initial phosphate concentrations. The Langmuir and Freundlich equations were used to fit the data of phosphate adsorption isotherms [29]. The linear forms of the Langmuir and Freundlich equations are expressed as Eq. (2) and Eq. (3), respectively:

$$C_e/Q_e = (1/Q_{max}) \times C_e + 1/(Q_{max} \times K_L) \quad (2)$$

$$\log Q_e = (1/n) \times \log C_e + \log K_F \quad (3)$$

where $Q_e$ (mmol $kg^{-1}$) is the quantity of phosphate adsorbed; $C_e$ (mmol $L^{-1}$) is the concentration of phosphate in the equilibrium solution; $Q_{max}$ is the maximum adsorption capacity of phosphate; and $K_L$ is the Langmuir adsorption constant related to the binding strength of phosphate on the surface of the Al (oxy) hydroxides. $K_F$ and $n$ are the Freundlich constants, which represent the adsorption capacity and intensity, respectively. The maximum adsorption capacities of phosphate on Al (oxy)hydroxides formed with and without pectin, as obtained from the Langmuir equation, were 248.2 mmol $kg^{-1}$ and 134.7 mmol $kg^{-1}$,

Table 1. Fitting parameters of the Langmuir and Freundlich equations for the adsorption isotherms of phosphate on aluminum hydroxides formed without pectin (control) and incorporating pectin at pH 5.5.

| | Langmuir | | | Freundlich | | |
|---|---|---|---|---|---|---|
| | $Q_{max}$ | $K_L$ | $R^2$ | n | $K_F$ | $R^2$ |
| Control | 134.7 | 13.14 | 0.995 | 8.99 | 120.2 | 0.984 |
| Incorporation of pectin | 248.2 | 9.37 | 0.984 | 5.38 | 210.3 | 0.990 |

respectively (Table 1). Pectin incorporation increased the maximum adsorption capacity of the Al (oxy) hydroxides for phosphate. Similarly, the values of $K_F$ obtained from the Freundlich equation were greater for the pectin-incorporating sample than for the control (Table 1). Incorporation of pectin decreased the $K_L$ of the Langmuir equation and *n* of the Freundlich equation. Therefore, although incorporating pectin resulted in an increase in the amount of phosphate adsorbed on Al (oxy)hydroxides, it decreased the binding strength.

## Phosphate Adsorption Kinetics

Kinetic studies are of great importance in delineating the processes and parameters that govern the fate of species in the environment [30]. Phosphate adsorption kinetics was studied in order to ascertain the factors controlling the rate of adsorption, potentially providing profound insight into the adsorption process [31]. The phosphate adsorption process on Al (oxy)hydroxides formed without the incorporation of pectin was initially rapid (120 min), but thereafter increased only slowly until a plateau of adsorption equilibrium was reached. In contrast, the phosphate adsorption process on Al (oxy)hydroxides incorporating pectin increased more slowly, but the adsorption amount exceeded that on the control after 120 min (Fig. 7a).

Three further kinetic models, namely pseudo-first-order [Eq. (4)], pseudo-second-order [Eq. (5)], and the Elovich equation [Eq. (6)], were used to describe the adsorption kinetics [32]:

$$q_t = q_1 \times (1 - e^{-K_1 \times t}) \quad (4)$$

$$t/q_t = 1/(K_2 \times q_2^2) + t/q_2 \quad (5)$$

$$q_t = \frac{1}{\beta} \times \ln(\alpha \times \beta) + \frac{1}{\beta} \times \ln t \quad (6)$$

where $q_1$ and $q_t$ are the amounts of phosphate adsorbed on the Al (oxy)hydroxides at equilibrium and at time *t* (mmol $kg^{-1}$), respectively, and $k_1$ is the rate constant ($min^{-1}$) of the pseudo-first-order model for the adsorption process; $q_2$ is the maximum adsorption capacity (mmol $kg^{-1}$) and $k_2$ is the rate constant (kg $mmol^{-1}$ $min^{-1}$) for the pseudo-second-order model; α is the initial adsorption rate (mmol $kg^{-1}$ $min^{-1}$) and β is the desorption constant (kg $mmol^{-1}$) for the Elovich model. The kinetic parameters of phosphate adsorption on Al (oxy)hydroxides formed with and without incorporation of pectin were calculated with Origin 8.5 software (OriginLab, Northampton, MA) and are listed in Table 2.

The pseudo-second-order model fitted the experimental data for the phosphate adsorption process on Al (oxy)hydroxides formed both with and without incorporation of pectin (Table 2). This implies that phosphate adsorption is a chemisorption process, which may involve a chemical reaction between $PO_4^{3-}$ and functional groups on the Al (oxy)hydroxides surface [31, 33]. This was further indicated by the release of hydroxyl during the kinetic experiments (Fig. 7b).

The rate constant ($k_2$) for the pseudo-second-order model decreased from $2.1612\times10^{-3}$ kg $mmol^{-1}$ $min^{-1}$ for the control to $2.599\times10^{-5}$ kg $mmol^{-1}$ $min^{-1}$ for the pectin-incorporating sample (Table 2). Incorporation of pectin decreased the positive charge on the hydroxides (Fig. 4) and thus increased the electrostatic repulsion between Al (oxy)hydroxides and phosphate, although phosphate was mainly adsorbed by the Al (oxy) hydroxides by chemical adsorption [34]. Therefore, phosphate could more easily reach the surface of the Al hydrolysis product formed without incorporation of pectin compared to that with pectin.

The maximum adsorption capacity ($q_2$) based on the pseudo-second-order model was increased from 71.942 mmol $kg^{-1}$ for the control to 192.308 mmol $kg^{-1}$ for the pectin-incorporating sample (Table 2). These results are also consistent with those derived from the phosphate adsorption isotherms. This suggests that the

Table 2. Kinetic parameters for the adsorption of phosphate on Al (oxy)hydroxides formed without and with incorporation of pectin.

| Kinetics model | Parameter | Control | Incorporation of pectin |
|---|---|---|---|
| Pseudo first order | $k_1$ ($min^{-1}$) | 0.41077 | 0.00453 |
| | $q_1$ (mmol $kg^{-1}$) | 64.516 | 154.6 |
| | $R^2$ | 0.8466 | 0.9890 |
| Pseudo second order | $k_2$ (kg $mmol^{-1}$ $min^{-1}$) | $2.1612\times10^{-3}$ | $2.599\times10^{-5}$ |
| | $q_2$ (mmol $kg^{-1}$) | 71.942 | 192.308 |
| | $R^2$ | 0.9982 | 0.9745 |
| Elovich quation | α (mmol $kg^{-1}$ $min^{-1}$) | 16246 | 4.4996 |
| | β (kg $mmol^{-1}$) | 0.19887 | 0.03583 |
| | $R^2$ | 0.9790 | 0.90702 |

adsorption rate of phosphate is mostly dependent on the availability of adsorption sites on the surface of the Al (oxy)hydroxides [35]. Two mechanisms can be envisaged for the pectin-enhanced adsorption of phosphate on Al (oxy)hydroxides. First, XRD and SEM analyses have indicated that the incorporation of pectin interferes with the formation of crystalline Al (oxy)hydroxides (Fig. 1 and Fig. 2). As has been reported, the phosphate adsorption capacity of synthesized non-crystalline Al/Fe hydroxides materials increases with decreasing structural ordering [36]. Secondly, phosphate can compete with pectin incorporated in poorly crystalline aluminum hydroxides. This is similar to the situation whereby phosphate may mobilize arsenate more easily from mixed iron-aluminum matrices rich in aluminum [37, 38].

The results showed that the pseudo-first-order model better fitted the experimental data for the phosphate adsorption process on Al (oxy)hydroxides formed by the incorporation of pectin, suggesting that the adsorption process mainly depends on the equilibrium phosphate concentration in the solution [35]. The results also showed that the Elovich model better fitted the experimental data for the phosphate adsorption process on Al (oxy)hydroxides formed without incorporation of pectin, corresponding to the chemical adsorption of phosphate on Al (oxy)hydroxides [39].

## Conclusions

XRD, SEM, and FTIR spectroscopic analyses have confirmed that the incorporation of pectin suppresses the crystallization of Al hydrolysis products, thereby introducing defects in their structure. The incorporation of pectin decreases the positive charge and the PZSE of Al (oxy)hydroxides, thereby enhancing the adsorption of phosphate thereon. The amount of phosphate adsorbed on Al hydrolysis products incorporating pectin is considerably higher than that on those formed without pectin at the same pH within the range 4.5-6.0. Although incorporating pectin increases the phosphate adsorption capacity, it decreases the binding strength of phosphate on Al (oxy)hydroxides. The incorporation of pectin decreases the rate constant and increases the maximum adsorption capacity of phosphate on the surface of Al (oxy)hydroxides. In conclusion, the incorporation of pectin affects the charge properties of Al (oxy)hydroxides, and the perturbation of Al hydrolysis products leads to poor crystallization, which increases the adsorption of phosphate.

## Acknowledgments

This study was supported by the National Natural Science Foundation of China (41571233，31670615 and 31270680), and the CAS Key Technology Talent Program.

## Conflict of Interest

The authors declare no conflict of interest.

## References

1. SIGUA G.C., STONE K.C., BAUER P.J., SZOGI A.A., SHUMAKER P.D. Impacts of irrigation scheduling on pore water nitrate and phosphate in coastal plain region of the United States. Agric. Water Manage. **186**, 75, **2017**.
2. NISHIGAKI T., TSUJIMOTO Y., RAKOTOSON T., RABENARIVO M., ANDRIAMANANJARA A., ASAI H., ANDRIANARY H.B., RAKOTONINDRINA H., RAZAFIMBELO T. Soil phosphorus retention can predict responses of phosphorus uptake and yield of rice plants to P fertilizer application in flooded weathered soils in the central highlands of Madagascar. Geoderma. **402**, 115326, **2021**.
3. LI Z., ZHANG R., LIU C., ZHANG R., CHEN F., LIU Y. Phosphorus spatial distribution and pollution risk assessment in agricultural soil around the Danjiangkou reservoir, China. Sci Total Environ. **699**, 134417, **2020**.
4. WANG M., ZHENG Y.M., LI Q., QI Y.Z., LIAO X., FU Q.C. The Efficiency Adsorption of Ammonia Nitrogen, Phosphate and Basic Blue 3 by Fulvic Acid Decorated $Fe_3O_4$ Magnetic Nanocomposites. Pol. J. Environ. Stud. **30** (4), 3299, **2021**.
5. BABOSOVA M., PORHAJASOVA J.I., CERYOVA T. Spatial and Seasonal Changes in Total and Phosphate Phosphorus Concentrations in the Water of National Nature Reserve Cicov Oxbow in the Southwestern Part of the Slovak Republic. Pol. J. Environ. Stud. **30** (4), 3481, **2021**.
6. WANG L., ZHAO X., GAO J.X., BUTTERLY C.R., CHEN Q.H., LIU M.Q., YANG Y.W., XI Y.G., XIAO X.J. Effects of fertilizer types on nitrogen and phosphorous loss from rice-wheat rotation system in the Taihu Lake region of China. Agric Ecosyst Environ. **285**, 106605, **2019**.
7. POMMERENK P., SCHAFRAN G.C. Adsorption of inorganic and organic ligands onto hydrous aluminum oxide: Evaluation of surface charge and the impacts on particle and NOM removal during water treatment. Environ. Sci. Technol. **39** (17), 6429, **2005**.
8. XU T.Y., WANG Q.H., WANG Z.M., CATALANO J.G. Effects of Phosphate Competition on Arsenate Binding to Aluminum Hydroxide Surfaces. Acs Earth And Space Chemistry. **5** (11), 3140, **2021**.
9. VIOLANTE A., MORA M.D., CAPORALE A.G. Formation, properties and reactivity of coprecipitates and organomineral complexes in soil environments. Journal of Soil Science and Plant Nutrition. **17** (2), 319, **2017**.
10. KWONG K.F.N.K., HUANG P.M. Sorption of Phosphate by Hydrolytic Reaction-Products of Aluminum. Natur. **271** (5643), 336, **1978**.
11. SINGER A., HUANG P.M. Effects of Humic-Acid on the Crystallization of Aluminum Hydroxides. Clays Clay Miner. **38** (1), 47, **1990**.
12. HU Y.F., XU R.K., DYNES J.J., BLYTH R.I.R., YU G., KOZAK L.M., HUANG P.M. Coordination nature of aluminum (oxy)hydroxides formed under the influence of tannic acid studied by X-ray absorption spectroscopy. Geochim. Cosmochim. Acta. **72** (8), 1959, **2008**.
13. XU R.K., HU Y.F., DYNES J.J., ZHAO A.Z., BLYTH R.I.R., KOZAK L.M., HUANG P.M. Coordination nature

of aluminum (oxy)hydroxides formed under the influence of low molecular weight organic acids and a soil humic acid studied by X-ray absorption spectroscopy. Geochim. Cosmochim. Acta. **74** (22), 6422, **2010**.
14. YU G., SAHA U.K., KOZAK L.M., HUANG P.M. Combined effects of tannate and ageing on structural and surface properties of aluminum precipitates. Clays Clay Miner. **55** (4), 369, **2007**.
15. YU G., SAHA U.K., KOZAK L.M., HUANG P.M. Kinetics of cadmium adsorption on aluminum precipitation products formed under the influence of tannate. Geochim. Cosmochim. Acta. **70** (20), 5134, **2006**.
16. XU R.K., YU G., KOZAK L.M., HUANG P.M. Desorption kinetics of arsenate adsorbed on Al (oxy)hydroxides formed under the influence of tannic acid. Geoderma. **148** (1), 55, **2008**.
17. FIRMANO R.F., COLZATO M., ALLEONI L.R.F. Phosphorus speciation and distribution in a variable-charge Oxisol under no-till amended with lime and/or phosphogypsum for 18 years. Eur. J. Soil Sci. **73** (1), **2021**.
18. CHEN Y.M., CHIU C.Y., TSAO T.M., LIU C.C., HUANG P.M., WANG M.K. Adsorption of Cadmium on Aluminum Precipitates in the Absence or Presence of Catechins. Sep. Sci. Technol. **48** (4), 598, **2013**.
19. LIU M.P., LI J., ZONG W., SUN W.W., MO W.J., LI S.F. Comparison of calcium and ultrasonic treatment on fruit firmness, pectin composition and cell wall-related enzymes of postharvest apricot during storage. Journal of Food Science and Technology-Mysore. **59** (4), 1588, **2022**.
20. DIAKITE M.S., LENORMAND H., LEQUART V., ARUFE S., MARTIN P., LEBLANC N. Cell Wall Composition of Hemp Shiv Determined by Physical and Chemical Approaches. Molecules. **26** (21), 6334, **2021**.
21. HUANG J.Y., LIAO J.S., QI J.R., JIANG W.X., YANG X.Q. Structural and physicochemical properties of pectin-rich dietary fiber prepared from citrus peel. Food Hydrocolloids. **110**, 106140, **2021**.
22. WANG R.H., ZHU X.F., QIAN W., YU Y.C., XU R.K. Effect of pectin on adsorption of Cu(II) by two variable-charge soils from southern China. Environmental Science and Pollution Research. **22** (24), 19687, **2015**.
23. WANG R.H., ZHU X.F., QIAN W., ZHAO M.H., XU R.K., YU Y.C. Adsorption of Cd(II) by two variable-charge soils in the presence of pectin. Environmental Science and Pollution Research. **23** (13), 12976, **2016**.
24. WANG R.H., ZHU X.F., QIAN W., HONG Z.N., TANG H.Y., XU R.K., YU Y.C. Pectin adsorption on amorphous Fe/Al hydroxides and its effect on surface charge properties and Cu(II) adsorption. J. Soils Sed. **17** (10), 2481, **2017**.
25. MU OZ-ALMAGRO N., MONTILLA A., MORENO F.J., VILLAMIEL M. Modification of citrus and apple pectin by power ultrasound: Effects of acid and enzymatic treatment. Ultrason. Sonochem. **38**, 807, **2017**.
26. HU S., WANG J., NIE S., WANG Q., XU X. Chain conformations and steady-shear viscosity properties of pectic polysaccharides from apple and tomato. Food Chemistry: X. **14**, 100296, **2022**.
27. LIU X.B., LU S., TANG Z., WANG Z.J., HUANG T.Y. Removal of sulfate from aqueous solution using Mg-Al nano-layered double hydroxides synthesized under different dual solvent systems. Nanotechnology Reviews. **10** (1), 117, **2021**.
28. ZHUANG J.S., LI M., PU Y.Q., RAGAUSKAS A.J., YOO C.G. Observation of Potential Contaminants in Processed Biomass Using Fourier Transform Infrared Spectroscopy. Applied Sciences-Basel. **10** (12), 4345, **2020**.
29. HILBRANDT I., LEHMANN V., ZIETZSCHMANN F., RUHL A.S., JEKEL M. Quantification and isotherm modelling of competitive phosphate and silicate adsorption onto micro-sized granular ferric hydroxide. Rsc Advances. **9** (41), 23642, **2019**.
30. PALMA G., DEMANET R., JORQUERA M., MORA M.L., BRICENO G., VIOLANTE A. Effect of pH on sorption kinetic process of acidic herbicides in a volcanic soil. Journal of Soil Science and Plant Nutrition. **15** (3), 549, **2015**.
31. PALANSOORIYA K.N., KIM S., IGALAVITHANA A.D., HASHIMOTO Y., CHOI Y.E., MUKHOPADHYAY R., SARKAR B., OK Y.S. Fe(III) loaded chitosan-biochar composite fibers for the removal of phosphate from water. J. Hazard. Mater. **415**, 125464, **2021**.
32. SPIRIDON I., APOSTOL I., ANGHEL N.C., ZALTARIOV M.F. Equilibrium, kinetic, and thermodynamic studies of new materials based on xanthan gum and cobalt ferrite for dye adsorption. Appl. Organomet. Chem., e6670, **2022**.
33. WANG S.D., KONG L.J., LONG J.Y., SU M.H., DIAO Z.H., CHANG X.Y., CHEN D.Y., SONG G., SHIH K.M. Adsorption of phosphorus by calcium-flour biochar: Isotherm, kinetic and transformation studies. Chemosphere. **195**, 666, **2018**.
34. MAYAKADUWAGE S., MOSLEY L.M., MARSCHNER P. Threshold for labile phosphate in a sandy acid sulfate soil. Geoderma. **371**, **2020**.
35. MANDAL A., SINGH N. Kinetic and isotherm error optimization studies for adsorption of atrazine and imidacloprid on bark of Eucalyptus tereticornis L. Journal of Environmental Science and Health Part B-Pesticides Food Contaminants and Agricultural Wastes. **51** (3), 192, **2016**.
36. ZHANG X., YAO H., LEI X., LIAN Q., ROY A., DOUCET D., YAN H., ZAPPI M.E., GANG D.D. A comparative study for phosphate adsorption on amorphous FeOOH and goethite (alpha-FeOOH): An investigation of relationship between the surface chemistry and structure. Environ Res. **199**, 111223, **2021**.
37. TIBERG C., SJOSTEDT C., ERIKSSON A.K., KLYSUBUN W., GUSTAFSSON J.P. Phosphate competition with arsenate on poorly crystalline iron and aluminum (hydr)oxide mixtures. Chemosphere. **255**, 126937, **2020**.
38. ZANZO E., BALINT R., PRATI M., CELI L., BARBERIS E., VIOLANTE A., MARTIN M. Aging and arsenite loading control arsenic mobility from ferrihydrite-arsenite coprecipitates. Geoderma. **299**, 91, **2017**.
39. TEGLADZA I.D., XU Q.L., XU K., LV G.J., LU J. Electrocoagulation processes: A general review about role of electro-generated flocs in pollutant removal. Process Saf. Environ. Prot. **146**, 169, **2021**.